OMAE2019-95068

THE AVERAGE SHAPE OF LARGE WAVES IN THE NORWEGIAN SEA – IS NON-LINEAR PHYSICS IMPORTANT?

Tianning Tang
University of Oxford
Oxford, UK
Email: tianning.tang@some.ox.ac.uk

Margaret J. Yelland
National Oceanography Centre,
Southampton, UK

Thomas A. A. Adcock
University of Oxford
Oxford, UK

ABSTRACT

   Linear wave theory predicts that in a random sea, the shape of the average wave is given by the scaled autocorrelation function — the "NewWave". However, the gravity wave problem is non-linear. Numerical simulations of waves on deep water have suggested that their average shape can become modified in a number of ways, including the largest wave in a group tending to move to the front of the group through non-linear dispersion. In this paper we examine whether this occurs for waves in the Norwegian Sea. Field data measured from the weather ship Polarfront is analysed for the period 2000 to 2009. We find that, at this location, the effect of non-linearity is small due to the moderate steepness of the sea-states.

NOMENCLATURE

H_s Significant wave height
t Time
T_z Zero-crossing period
s Steepness of the sea state
BFI Benjamin-Feir Index
Q_p Quality factor
f Frequency
f_p Peak frequency
η Surface elevation
α Relative wave crest height
B NewWave based relative envelope height half period away from peak
k_p Dominant wave number

d Water depth from the mean water level
g Gravitational acceleration
m_0 Zeroth moment of the variance density spectrum
S Variance density spectrum
η_p Preceding crest height
η_f Following crest height
η_{max} Maximum crest height
η_H Hilbert transformed elevation
U Wave envelope

INTRODUCTION

   There is much academic and engineering interest in the dynamics of extreme waves, sometimes called freak or rogue waves, in the open ocean [1–3]. In the present paper we focus on the shape of extreme events in the open ocean and how this may be modified relative to linear theory by non-linear physics. In a linear model of ocean waves, the expected shape of an extreme event is symmetrical and is essentially a scaled auto-correlation function (and thus dependent on the energy spectrum) [4–6]. A series of papers on isolated wave-groups [7–9] and random seas [10, 11] predicted that the expected shape in non-linear theory is slightly different with:

1. The largest wave moving to the front of the wave-group;
2. The group expanding in the lateral direction relative to linear theory;
3. The group contracting in the mean wave direction relative to linear theory.

These conclusions are somewhat contradicted by a recent numerical study by Fujimoto *et al.* [12] where more realistic ocean energy spectra are considered. Further work suggests that the changes predicted above are, to some extent, caused by spectra which are out of equilibrium and therefore these changes might be smaller in the open ocean.

The first paper to examine whether these changes can be observed in field measurements in the open ocean was by Gemmrich & Thomson [13]. They observed some small departures from linear theory for the steepest waves in apparent agreement with theory, although this is not what they concluded in their paper. Tang et al. have followed this with an analysis of waves on Lake George in Australia and the North Sea. They found significant non-linear physics present in the very steep and narrow-banded lake data, but only very small changes present in data measured in the North Sea, although these findings were consistent with theory.

In the present paper we extend the analysis of Tang *et al.* to a dataset measured in the Norwegian Sea. This is much deeper water than previous studies and a location which is exposed to a long fetch and therefore primarily to 'old' waves. The wave climate measured is severe with some large waves. However, the sea-states are generally not particularly steep or narrow-banded as would be expected from the location. We present some background analysis of the data and sea-states included in this study before analysing the data for asymmetry around the large waves and for departures in the length of an extreme wave group from linear theory.

DATA

This paper analyses the extreme gravity waves recorded by a weather ship at the Norwegian Sea. We first present a brief background information of the dataset in the first part, which is followed by some detailed parameters to fully describe the sea-state.

Description of Norwegian Sea Data

Surface elevation measurements of the Norwegian Sea are taken from *OWS Polarfront*, the last weather ship in the world, which was withdrawn from operation at Station Mike in late 2009. This weather ship has been monitoring the ocean environment, including wave statistics H_{max} (approximately the average height of the largest third of the waves) and H_{max} (the largest wave height recorded), for over thirty years using a Ship-Borne Wave Recorder (SBWR). This is a system developed by the UK National Institute of Oceanography and its operation principle is illustrated by Tucker and Pitt [14]. Over the past decades, research work has validated SBWR measurements and yielded the conclusion that the SBWR is a reliable system with relatively high accuracy. Graham *et al.* [15] validated the SBWR

measurements with the WaveRider buoy and found that although the significant wave height H_s of the sea-state is 8% larger than the buoy data, the extreme values, which are crucial for this paper, are fairly consistent. Clayson [16] performed another similar comparison between SBWR and a WaveRider buoy that was conducted specifically for this weather ship *(OWS Polarfront)*, which also showed a satisfactory consistency between these two methods. Moreover, after analysing the SBWR measurements in the Rockall Trough, Holliday [17] also concluded that the SBWR is an acceptable device for obtaining wave elevations in deep water.

The *OWS Polarfront* recorded wave environment for over thirty years. For the last ten years (2000-2009), the water elevation was recorded at a sampling frequency of 1.7 Hz for thirty-minute periods. The thirty-minute wave elevation record was taken for every ninety minutes between the start of 2000 and the 250th day of 2004. After that, the wave elevation was measured more frequently providing thirty-minutes of wave data for every sixty minutes. This dataset has been described fully in [18] and [19]. No significant influence was observed due to the change of sampling period for the last six years [20]. During this ten-year measurement campaign, free drift of the ship was allowed within a circle of 32 km in radius around the measurement site Mike (66°N, 2.2°E), which is shown in Fig. 1. If the ship crosses the boundary of the measurement site, the engine will drive the ship to return to the centre of the site. During the periods in which the engine was active, some abnormal freak waves are found and discarded. Apart from returning to the centre of the station, the ship returned to the harbour for three days out of every 28 days, which is recorded by the navigation files, and the recordings during this period are excluded from further analysis in this paper.

Besides rejecting certain time series due to ship movement and off-site positioning, more data are filtered out by a rigorous data quality control process following the approach of [21]. Additionally, the data with maximum elevation less than 1 m is also ignored in the following analysis to avoid relatively young waves created by strong local winds contaminating the results. A total of 70,971 thirty-minute time series have passed the quality control process and are used in this analysis. Although the water depth may vary a bit within the 32 km measurement site, the average water depth from the mean water level is over 2 km, which gives a relative water depth ($k_p d$) of a number always much larger than 3. Thus, all the waves we analyse herein are deep water waves.

Background Sea State

The background sea-state varies significantly during the measurement period, especially during winter, which leads to the significant wave height varying from 0.6 m to 15.18 m during the winter storm in Fig. 2. The maximum wave height during these extreme conditions could be as large as 25.57 m. The domi-
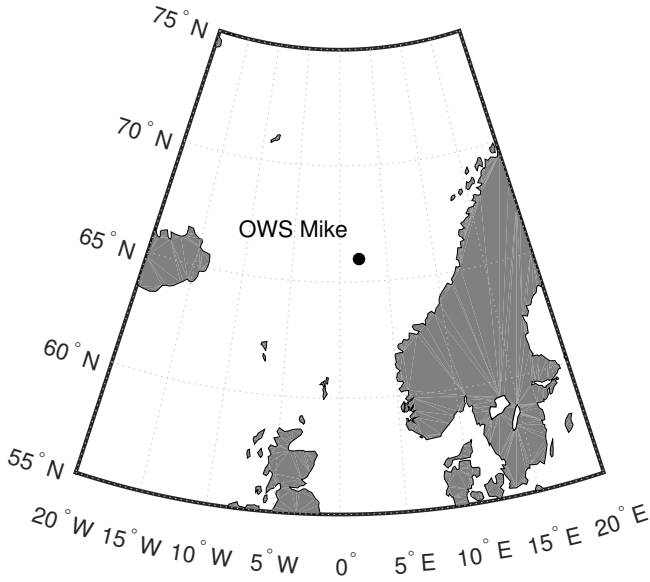
FIGURE 1. LOCATION OF OCEAN WATER STATION MIKE

nant frequency varies from 0.4 rad/s to 1.54 rad/s, which agrees with other field measurements in open ocean [21]. To examine the non-linearity of the background sea-state, lines of constant mean steepness of the sea-state are also presented in Fig. 2, where steepness is defined as

$$s = \frac{2\pi}{g} \frac{H_s}{T_z^2}. \tag{1}$$

From Fig. 2, the steepness values of the sea-state generally agrees with other field measurements.

Another important parameter for describing the non-linearity of the sea-state is the Benjamin-Feir Index (BFI) introduced by Janssen [22]. Although the BFI is not a perfect parameter for measuring the non-linearity (it does not contain any information on directional spreading, which is known to be important), it is closely associated with third order non-linear physics. To compute the BFI for random time series, we used the approach introduced by Serio *et al.* [23], which gives the BFI based on quality factor and steepness for deep water waves:

$$BFI = \sqrt{m_0} k_p Q_p \sqrt{2\pi}, \tag{2}$$

where m_0 can be computed as $H_s^2/16$. Q_p is the quality factor presented by Goda [24], which can provide an estimation of spectral bandwidth without being affected too much by the cutoff

frequency [25]. Q_p is given as:

$$Q_p = \frac{2}{m_0^2} \int_0^\infty f\, S^2(f)\, df. \tag{3}$$

A higher Q_p value indicates a narrow-banded spectrum. Based on Equation 2, we present the quality factor and steepness of the sea state for each time series in Figure 3 with constant lines of BFI. It is also remarkable that despite having several measurements with relatively high BFI values, no time series have a BFI value greater than 1, which is theoretically the critical value for wave stability [22, 26]. This result is consistent with the similar analyses of the waves in the North Sea and the Lake George.

Typical Spectrum

The wave spectrum is one of the most important tools for analysing the sea-state. The wave spectrum varies over time, and each individual time series has a unique wave spectrum. However, we believe it is still useful to present a typical omnidirectional wave spectrum from one time series with its zero-crossing period and significant wave height close to the mean value of the whole database, which is shown in Fig. 4. This spectrum could provide an insight into the energy distribution computed from a typical measured sea-state around the measurement site. To compute this spectrum, the time series is divided into 20 non-overlapping segments with a Tukey window before the Fast Fourier Transform to avoid spectral leakage. The final spectrum is then computed simply by averaging among all the segments to smooth the results. The final spectrum is also normalized by the
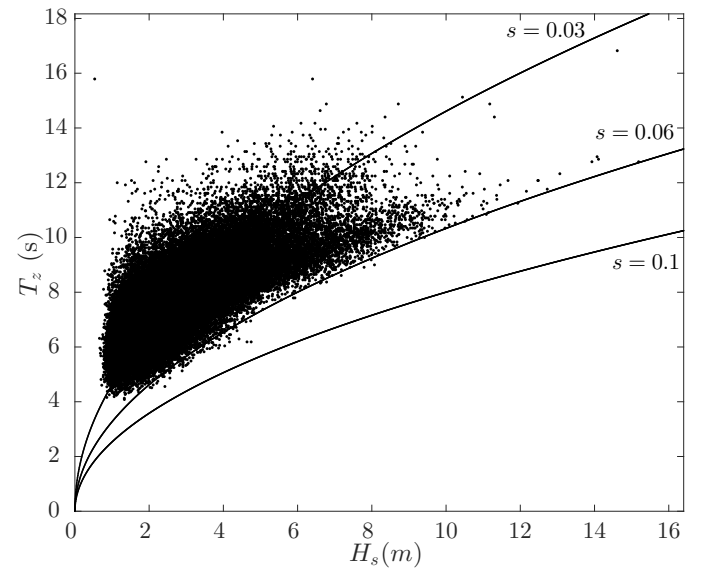

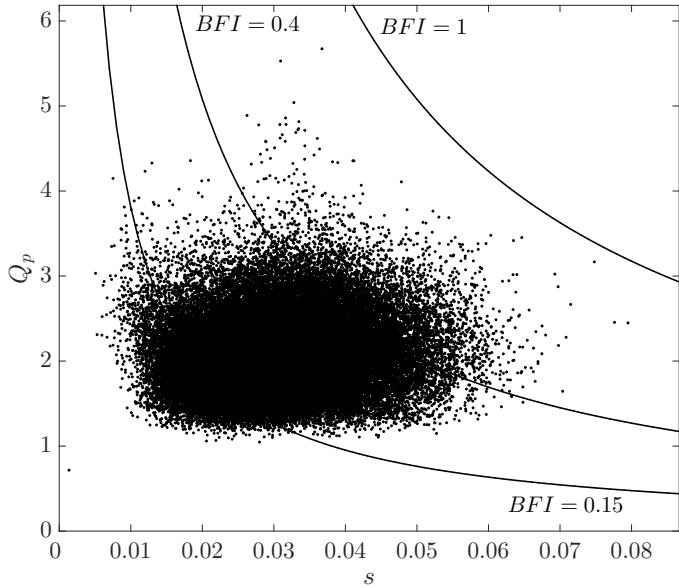**FIGURE 2**. SCATTER PLOT FOR H_s AND T_z

FIGURE 3. SCATTER PLOT FOR STEEPNESS AND QUALITY FACTOR

peak frequency of the individual time series.

Although the spectrum is similar to the typical spectrum computed from open ocean around the peak frequency and high frequency tail, the energy in the low frequency range is significantly larger than the typical spectrum reported by other Eulerian field measurements [27, 28]. This could be due to the data analysed here being captured by the SBWR, which is a semi-
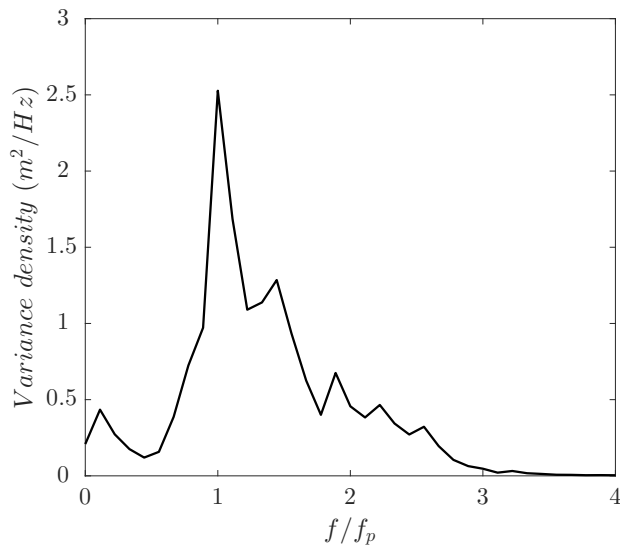

FIGURE 4. TYPICAL SPECTRUM

Lagrangian measuring device. As the ship itself will tend to move with the wave, the SBWR installed on the both sides of the boat cannot provide accurate Eulerian measurements of the surface elevation. Instead, some characteristics reported in Lagrangian measurements such as an absence of the second order sum term and greatly amplified difference interactions [29, 30] can be found in the time series. This also leads to most of the time series in the dataset having negative skewness, which makes the linearization process following the approach of [31] extremely difficult. Hence, the results we present in this paper include some of the bound wave effects.

Apart from the relative bandwidth and steepness, directional spreading is also a key factor for the impact of non-linear physics on open ocean waves. Unfortunately, due to the limitation of the measuring device, there is no directional information available in the database analysed in this paper. Although there is some directional information that can be inferred from an Eulerian point measurement [32, 33] the semi-Lagrangian nature of this database means the sub-harmonics cannot be extracted as clearly as required for this technique.

RESULTS

In this section, the horizontal asymmetry of the largest waves in each random time series will be investigated using two parameters: the relative crest height near the largest crest and the envelope height on either side of the envelope. Both parameters present the horizontal asymmetry of the largest waves in a slightly different aspect but both of them are closely related with the non-linearity of the background sea-state.

Analysis of Raw Time Series

We start by looking at the relatively raw time series but with proper quality control processes. This will help us to demonstrate that the results observed herein is not introduced by the post-processing procedure.

To access the horizontal asymmetry properties of the largest waves in each of the elevation time histories, we first find the top five largest crests/waves in each records. An additional check on this extraction procedure confirms that these largest waves must have a distance of at least two zero-crossing periods between them, which prevents analysing two crests from the same wave packet. Afterwards, the height of the preceding crest (η_p) and following crest (η_f) are calculated, which are then compared with the largest crest height (η_{max}) found previously. This gives the first parameter α for measuring the horizontal asymmetry of the field measurements and the non-linear impact on the average shape of the largest events as the linear theory (NewWave) [4–6]

4

predicts these to be symmetrical. The α is defined as:

$$\alpha_{preceding} = \frac{\eta_p}{\eta_{max}}, \ \alpha_{following} = \frac{\eta_f}{\eta_{max}}. \qquad (4)$$

All of the raw time series that have passed the quality control procedure are processed and the value of $\alpha_{preceding}$ and $\alpha_{following}$ are computed from the average shape of top five largest crests in each recording. These α values are then divided into several bins based on two main parameters of the background sea-state: steepness and the normalized maximum elevation (η_{max}/H_s), which is the ratio of the maximum elevation in each time series to the significant wave height. The steepness is an important parameter for describing the non-linearity of the sea-state, and the normalized maximum elevation presents the significance of the largest wave compared with the underlying sea-state. The average value of $\alpha_{preceding}$ and $\alpha_{following}$ in each bin are computed and presented in Fig 5. We have also computed the error bar based on the bootstrapping method [34] to provide a 90% confidence interval of the mean value in each bin.

In Fig. 5 (left), α is categorized by the normalized maximum elevation, which shows a clear separation between $\alpha_{preceding}$ and $\alpha_{following}$ for high normalized maximum elevation values. This indicates that the wave in the front of a large wave tends to be smaller than the one following it when the random time series contains sufficiently large waves compared to the background sea-state. However, this horizontal asymmetry is not very clear when there is no rogue waves (*i.e* large wave relative to the background sea-state) occurring within the time series. This tendency of horizontal asymmetry is consistent with the numerical simulation [10].

Furthermore, both $\alpha_{preceding}$ and $\alpha_{following}$ tend to decrease for higher normalized crest height, which suggests a larger wave tends to have both smaller relative preceding crest height and following wave height. This might be due to the non-linear contraction of the wave envelope but could also simply be due to the bound harmonics. As mentioned in the previous section, we find it rather difficult to linearize the data; thus no simple conclusion can be drawn from this trend.

In Fig. 5 (right), all $\alpha_{preceding}$ and $\alpha_{following}$ values are divided into different bins based on the steepness of the sea-state. For the mild sea-states, the difference between $\alpha_{preceding}$ and $\alpha_{following}$ is minimal. Horizontal asymmetry only appears at relatively steep sea-states, which indicates this horizontal asymmetry is closely related with non-linear physics. There is no clear correlation between α and steepness, which may due to the bound harmonics. Both the overall trend and the detailed value of α shown in Fig. 5 are quite similar with the data captured in the North Sea, which further suggests that horizontal asymmetry can be found in the open ocean.

For the behaviour of large waves, the $\alpha_{preceding}$ and

$\alpha_{following}$ values for wave records with H_s larger than 6 m is also presented in Fig. 6 as these are the waves which are most significant for offshore engineering. From Fig. 6, the horizontal asymmetry is still clear for relative high normalized maximum crest height and steepness. However, the overall tendency is less significant due to the significant decrease in the total number of wave records analysed.

Analysis of Envelope

To further investigate the horizontal asymmetry shown in the previous subsection, the horizontal asymmetry properties of the envelope is examined herein. The envelope of a random time series can be obtained following the approach of [35]:

$$|U| = \sqrt{\eta^2 + \eta_H^2}. \qquad (5)$$

To examine the asymmetric properties of the envelope, the envelope profiles of the top five largest waves are calculated and normalized by the maximum envelope height. Due to this dataset having a relatively low sampling frequency, an up-sampling procedure was performed with a high order polynomial fit. The best fit line were carefully compared with raw data to avoid introducing extra error into further analysis. The envelope profiles are then averaged within each individual time series. However, the shape of these envelopes are influenced by the underlying spectrum of the sea-state. Hence, these envelopes are compared with envelopes based on the expected shape of an extreme event in linear theory (NewWave) [4–6] to ensure that any observed trend is not due to the correlations between steepness and bandwidth. The NewWave profile with unity amplitude is given as:

$$\eta(t) = \frac{1}{m_0} \int_0^\infty S(f)\cos(2\pi f t)\mathrm{d}f. \qquad (6)$$

During this calculation, an assumption is made that the measured spectrum can be approximated as the linear spectrum due to the difficulties in linearizing the field data. To investigate the difference between the measured envelope and the envelope predicted by the linear theory, the height of the averaged envelope at a distance of a half zero-crossing period away from the maximum envelope position on both sides are computed as $|U|_{preceding}$ and $|U|_{following}$ for both measured envelope (see Fig. 7 as an example) and NewWave envelope. A parameter B is introduced to quantify the difference between measured envelope and NewWave envelope for each time series, which is defined as:
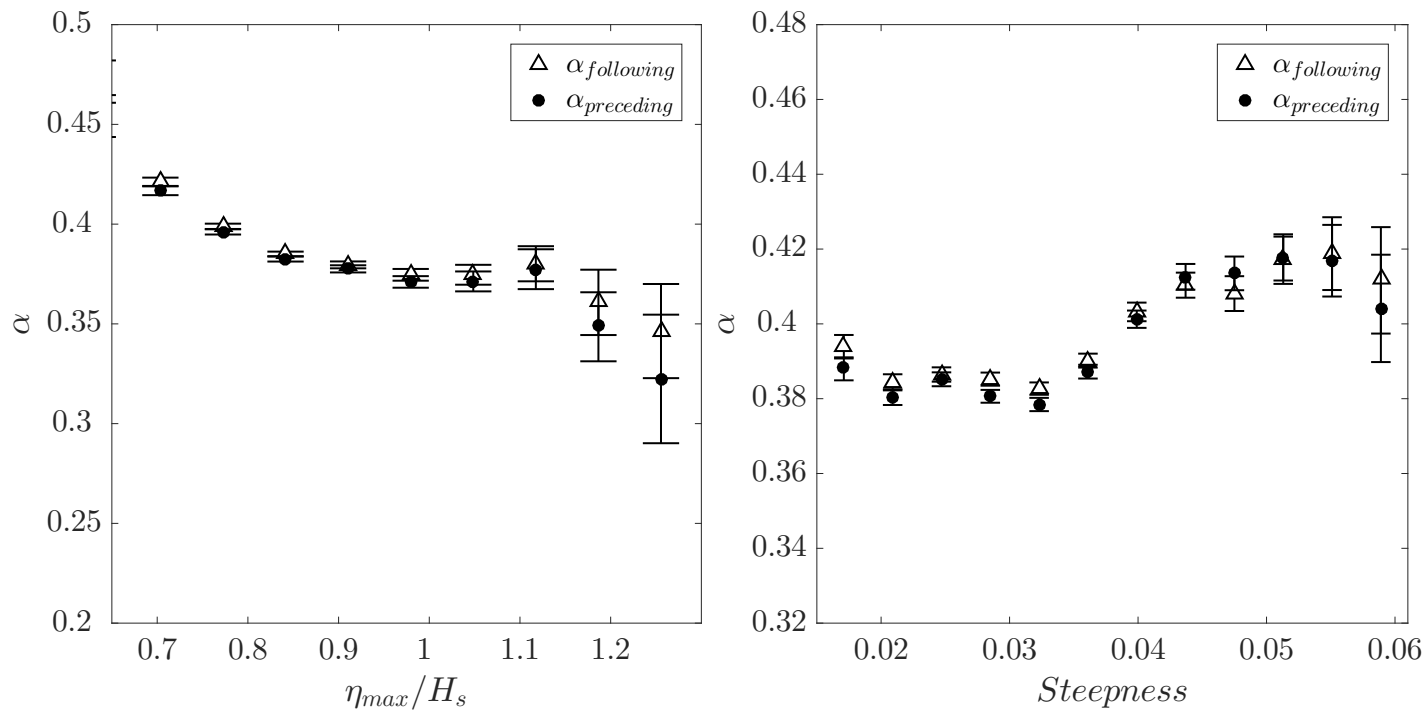
FIGURE 5. RELATIVE WAVE HEIGHT OF PRECEDING AND FOLLOWING CRESTS AGAINST LEFT: NORMALIZED MAXIMUM ELEVATION, RIGHT: STEEPNESS
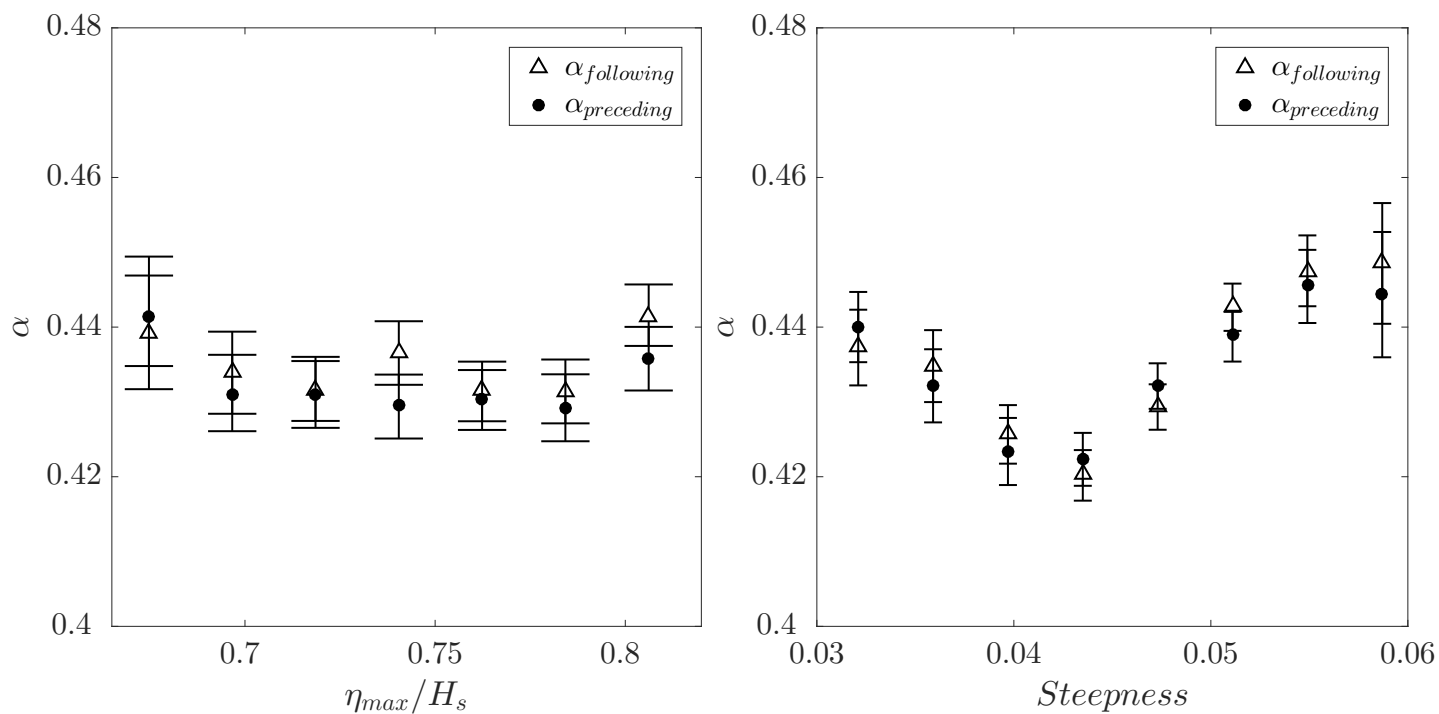

FIGURE 6. RELATIVE WAVE HEIGHT OF PRECEDING AND FOLLOWING CRESTS AGAINST LEFT: NORMALIZED MAXIMUM ELEVATION, RIGHT: STEEPNESS FOR WAVE RECORDS WITH H_s LARGER THAN 6 M

6

$$B_{preceding} = \frac{|U|_{preceding,measured}}{|U|_{preceding,NewWave}},$$

$$B_{following} = \frac{|U|_{following,measured}}{|U|_{following,NewWave}}. \quad (7)$$

In Fig. 8 (left), the NewWave-based relative envelope height B is categorized based on the mean steepness of the sea-state. The difference between preceding and following envelope heights at half zero-crossing period away is clear. As the NewWave envelope is always symmetrical about the maximum envelope position, the observed difference suggests that the measured envelope tends to have a steeper front and a flat tail, which further confirms that horizontal asymmetry can be found in the open ocean. Additionally, this horizontal asymmetry is enhanced by the mean steepness of the sea-state as the difference between preceding envelope height and following envelope height greatly increases for higher steepness in Fig. 8. This suggests that the horizontal asymmetry properties of open ocean waves are greatly dependent on the non-linearity of the sea-state, which also agrees well with the previous numerical simulation [10].

All the B values in Fig 8 (left) are quite close to 1, which suggests NewWave is still a good approximation for extreme events in the open ocean, which agrees well with previous findings [36]. However, the change in the group bandwidth relative to that predicted by linear theory and described in [9] is not observed in Fig. 8. To further investigate this property, the mean value of NewWave-based relative envelope height B_{mean} is calculated for
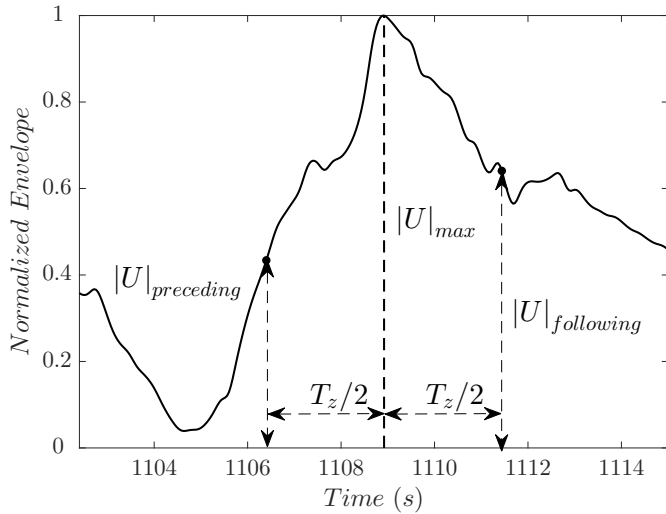
both measured envelope and NewWave envelope as:

$$B_{mean} = \frac{|U|_{preceding,measured} + |U|_{following,measured}}{|U|_{preceding,NewWave} + |U|_{following,NewWave}}. \quad (8)$$

In Fig. 8 (right), the mean value of B_{mean} is categorized by the mean steepness of the background sea-state. From Fig. 8 (right), the ratio between the mean value of the envelope height are close to unity for the sea-state with low steepness, which indicates there is no significant contraction in the mean wave direction and NewWave captures the group bandwidth accurately. However, there is a slight decreasing trend in B_{mean} values at relatively high steepness cases, which indicates the measured envelope tends to contract when the background sea-state is more non-linear. This trend is not as significant as the previous numerical simulations [11] and field measurements, the discrepancy might be due to the parameter introduced here being quite sensitive to bound harmonics, which is found to be difficult to exclude from the analysis.

DISCUSSIONS

In this paper, we have investigated the asymmetric properties of large random waves in the Norwegian sea. We found that, on average, the wave in front of a large wave is smaller than the wave coming after it. In our view, the most probable explanation of this phenomenon is due to the non-linear dispersion relationship, in which, the largest wave tends to travel faster than the small wave and hence moves to the front of the wave group. This non-linear physics has been explored by Adcock *et al.* [10] with numerical simulations for realistic directional spread seas. Additionally, the asymmetry observed in these data is also closely related with the mean steepness of the sea state, which agrees well with numeric results [8, 10] and further confirms that this phenomenon is closely related with non-linear physics.

We have also analysed the change in the shape of the envelope of large events. We found that the envelope of large events generally has a steep front and a flat tail when compared to the envelope predicted by the linear theory. This tendency is also more significant in the sea-state with relatively high steepness. This further supports the asymmetric property found previously between the preceding wave and following wave and its correlation with the steepness of the sea-state in terms of the raw time series.

Additionally, the change in the mean envelope height at a distance of half zero-crossing period away from the maximum point is also investigated. The results show some minor decreases in the mean envelope height at relatively high steepness, which might suggest that the envelope contracts in the mean wave direction, although it is hard to say definitively. When
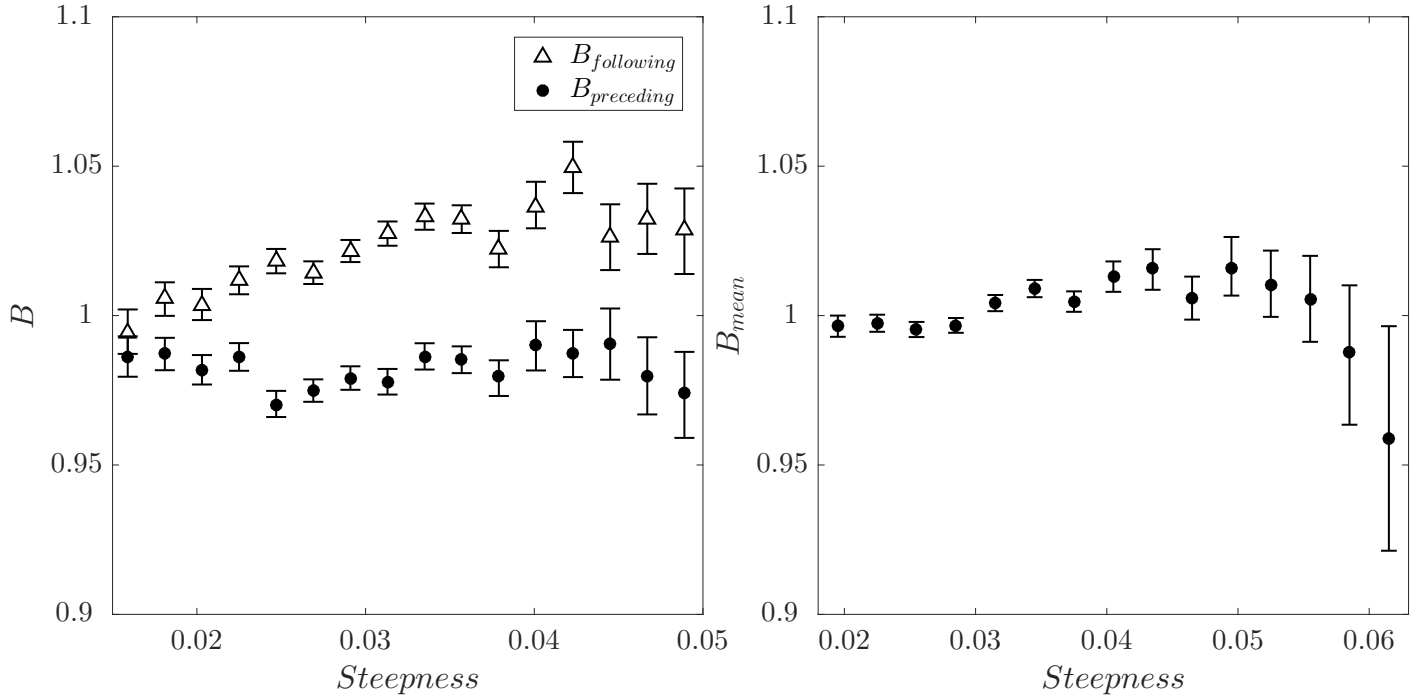

FIGURE 7. ILLUSTRATION OF THE RELATIVE ENVELOPE HEIGHT AT $T_z/2$ AWAY FROM THE ENVELOPE MAXIMUM

FIGURE 8. NEWWAVE BASED RELATIVE ENVELOPE HEIGHT HALF PERIOD AWAY FROM PEAK AGAINST STEEPNESS. LEFT: FOR PRECEDING AND FOLLOWING POSITIONS, RIGHT: FOR MEAN VALUE

compared with other field measurements and numerical predictions, the contraction in the mean wave direction is not as significant for this dataset.This may be due to the measurement method or because this phenomenon is not present in the dataset. One possible reason for the insignificant contraction can be that this dataset has relatively low steepness, when compared with severe winter storms in the North Sea [21]. The effects studied here are known to be very sensitive to non-linearity [11]. Additionally, semi-Lagrange data measurement leads to huge difficulties in eliminating the effects from bound harmonics, which may alter the shape of the measured envelope. Low sampling frequency also causes incomplete description of the elevation time series in the Norwegian sea, which could potentially have some impact on the calculated envelope. Based on these limits of the dataset, we cannot draw any solid conclusion in the change in the width of the envelope and influence of the bandwidth on this asymmetric property.

Apart from the non-linear dispersion relationship, there may be some other causes leading to the results we demonstrated in this paper. One possibility is the local wind/wave interactions, which is believed to have an impact on underlying Gaussian distribution [37, 38]. As strong local wind is also closely related with steep and narrow-banded sea-states, which happen to have huge impacts on asymmetric properties [3], we cannot rule out this effect; however, the impact from wind/wave interactions is

usually limited to a single crest [39]. A further possibility is that the asymmetry observed is in some way connected to the semi-Lagrange nature of the measurements.

Although there may be other causes that can lead to the results reported here, since the horizontal asymmetry has a strong correlation with the steepness and the results agree well with the numerical simulations [10], we are confident that non-linearity provides the most probable explanation for the results. Additionally, the statistics obtained from the large dataset also shows that the wave behaviour departs from that predicted by linear theory. However, due to the moderate steepness and the broader spectrum of the sea-states, the modifications from non-linear physics is small and can only be seen for steep sea-states and with a large amount of data available. For a location with spectra like those studied here, it would be reasonable to neglect this effect in engineering calculations. However, although small, we believe this is a robust feature for ocean waves since this phenomenon has been reported from different datasets in the open ocean. The broadening of the wave crest, which is predicted to occur in lower steepnesses [40], may be more common in the open ocean than the effect analysed in this paper and ultimately of more engineering importance.

REFERENCES

[1] Kharif, C., and Pelinovsky, E., 2003. "Physical mechanisms of the rogue wave phenomenon". *Eur. J. Mech.*, *22*(6), pp. 603–634.

[2] Dysthe, K., Krogstad, H. E., and Müller, P., 2008. "Oceanic Rogue Waves". *Annu. Rev. Fluid Mech.*, *40*(1), pp. 287–310.

[3] Adcock, T. A. A., and Taylor, P. H., 2014. "The physics of anomalous ('rogue') ocean waves". *Reports Prog. Phys.*, *77*(10), p. 105901.

[4] Boccotti, P., 1983. "Some new results on statistical properties of wind waves". *Appl. Ocean Res.*, *5*(3), jul, pp. 134–140.

[5] Lindgren, G., 1970. "Some Properties of a Normal Process Near a Local Maximum". *Ann. Math. Stat.*, *41*(6), pp. 1870–1883.

[6] Tromans, P. S., Anatruk, A. R., and Hagemeijer, P., 1991. "New Model for the Kinematics of Large Ocean Waves Application as a Design Wave". *Proc. First Int. Offshore Polar Eng. Conf.*, *8*(August), pp. 64–71.

[7] Johannessen, T. B., and Swan, C., 2001. "A laboratory study of the focusing of transient and directionally spread surface water waves". *Proc. R. Soc. London. Ser. A Math. Phys. Eng. Sci.*, *457*(2008), apr, pp. 971 LP – 1006.

[8] Gibbs, R. H., and Taylor, P. H., 2005. "Formation of walls of water in 'fully' nonlinear simulations". *Appl. Ocean Res.*, *27*(3), jun, pp. 142–157.

[9] Adcock, T. A. A., Gibbs, R. H., and Taylor, P. H., 2012. "The nonlinear evolution and approximate scaling of directionally spread wave groups on deep water". *Proc. R. Soc. A Math. Phys. Eng. Sci.*, *468*(2145), sep, pp. 2704 LP – 2721.

[10] Adcock, T. A. A., Taylor, P. H., and Draper, S., 2015. "Nonlinear dynamics of wave-groups in random seas: unexpected walls of water in the open ocean". *Proc. R. Soc. A Math. Phys. Eng. Sci.*, *471*(2184), dec.

[11] Adcock, T. A. A., Taylor, P. H., and Draper, S., 2016. "On the shape of large wave-groups on deep water—The influence of bandwidth and spreading". *Phys. Fluids*, *28*(10), oct, p. 106601.

[12] Fujimoto, W., Waseda, T., and Webb, A. "Impact of the four-wave quasi-resonance on freak wave shapes in the ocean". *Ocean Dynamics*, pp. 1–21.

[13] Gemmrich, J., and Thomson, J., 2017. "Observations of the shape and group dynamics of rogue waves". *Geophys. Res. Lett.*, *44*(4), feb, pp. 1823–1830.

[14] Tucker, M., and Pitt, E., 2001. *Waves in Ocean Engineering (Elsevier Ocean Engineering)*. Elsevier ocean engineering book series. Elsevier.

[15] Graham, C. G., Verboom, G., and Shaw, C. J., 1978. Comparison of Shipborne Wave Recorder and Waverider Buoy Data used to Generate Design and Operational Planning Criteria, may.

[16] Clayson, C. A., 1997. "Intercomparison between a WS Ocean Systems Ltd. Mk IV shipborne wave recorder (SWR) and a Datawell Waverider (WR) deployed from DNMI ship Polarfront during March-April 1997, Southampton Oceanography Centre, Southampton, UK. 26pp".

[17] Holliday, N. P., Yelland, M. J., Pascal, R., Swail, V. R., Taylor, P. K., Griffiths, C. R., and Elizabeth, K., 2006. "Were extreme waves in the Rockall Trough the largest ever recorded?". *Geophys. Res. Lett.*, *33*(5), mar.

[18] Yelland, M., Bjorheim, K., Gommenginger, C., Pascal, R. W., and Moat, B., 2007. "Future exploitation of in-situ wave measurements at station mike". *JCOMM Scientific and Technical Symposium on Storm Surges*, 10.

[19] Yelland, M., Holliday, N., Skjelvan, I., Østerhus, S., and J Conway, T., 2009. "Continuous observations from the weather ship polarfront at station mike".

[20] Feng, X., Tsimplis, M., Yelland, M., and Quartly, G., 2014. "Changes in significant and maximum wave heights in the Norwegian Sea". *Glob. Planet. Change*, *113*, feb, pp. 68–76.

[21] Christou, M., and Ewans, K., 2014. "Field Measurements of Rogue Water Waves". *J. Phys. Oceanogr.*, *44*(9), pp. 2317–2335.

[22] Janssen, P. A. E. M., 2003. "Nonlinear four-wave interactions and freak waves". *J. Phys. Oceanogr.*, *33*(4), pp. 863–884.

[23] Serio, M., Onorato, M., Osborne, A. R., and Janssen, P. A. E. M., 2005. "On the computation of the Benjamin-Feir Index". *Nuovo Cim. della Soc. Ital. di Fis. C*, *28*(6), nov, pp. 893–903.

[24] Goda, Y., 2000. *Random seas and design of maritime structures*, Vol. 15. World Scientific Publishing Co. Pte. Ltd, jan.

[25] Prasada Rao, C. x. K., 1988. "Spectral width parameter for wind-generated ocean waves". *Proc. Indian Acad. Sci. - Earth Planet. Sci.*, *97*(2), p. 173.

[26] Benjamin, T. B., and Feir, J. E., 1967. "The disintegration of wave trains on deep water Part 1. Theory". *J. Fluid Mech.*, *27*(3), pp. 417–430.

[27] Hwang, P. A., Fan, Y., Ocampo-Torres, F. J., and García-Nava, H., 2017. "Ocean Surface Wave Spectra inside Tropical Cyclones". *J. Phys. Oceanogr.*, *47*(10), jul, pp. 2393–2417.

[28] Santo, H., Taylor, P. H., Eatock Taylor, R., and Choo, Y. S., 2013. "Average Properties of the Largest Waves in Hurricane Camille". *J. Offshore Mech. Arct. Eng.*, *135*(1), feb, pp. 11602–11607.

[29] Longuet-Higgins, M. S., 1986. "Eulerian and lagrangian aspects of surface waves". *Journal of Fluid Mechanics*, *173*, p. 683–707.

[30] Herbers, T. H. C., and Janssen, T. T., 2016. "Lagrangian

surface wave motion and stokes drift fluctuations". *Journal of Physical Oceanography,* **46**(4), pp. 1009–1021.

[31] Walker, D. A. G., Taylor, P. H., and Eatock Taylor, R., 2004. "The shape of large surface waves on the open sea and the Draupner New Year wave". *Appl. Ocean Res.,* **26**(3-4), may, pp. 73–83.

[32] Adcock, T. A. A., and Taylor, P. H., 2009. "Estimating ocean wave directional spreading from an Eulerian surface elevation time history". *Proc. R. Soc. A Math. Phys. Eng. Sci.,* **465**(2111), pp. 3361–3381.

[33] McAllister, M. L., Adcock, T. A. A., Taylor, P. H., and van den Bremer, T. S., 2018. "The set-down and set-up of directionally spread and crossing surface gravity wave groups". *J. Fluid Mech.,* **835**, pp. 131–169.

[34] Efron, B., and Tibshirani, R. J., 1994. *An introduction to the bootstrap*. CRC press.

[35] Janssen, P. A. E. M., 2014. "On a random time series analysis valid for arbitrary spectral shape". *Journal of Fluid Mechanics,* **759**, p. 236–256.

[36] Jonathan, P., and Taylor, P. H., 1997. "On Irregular, Nonlinear Waves in a Spread Sea". *J. Offshore Mech. Arct. Eng.,* **119**(1), feb, pp. 37–41.

[37] Kharif, C., Giovanangeli, J.-P., Touboul, J., Grare, L., and Pelinovsky, E., 2008. "Influence of wind on extreme wave events experimental and numerical approaches". *J. Fluid Mech.,* **594**, pp. 209–247.

[38] Toffoli, A., Proment, D., Salman, H., Monbaliu, J., Frascoli, F., Dafilis, M., Stramignoni, E., Forza, R., Manfrin, M., and Onorato, M., 2017. "Wind generated rogue waves in an annular wave flume". *Phys. Rev. Lett.,* **118**(14), p. 144503.

[39] Agnon, Y., Babanin, A. V., Young, I. R., and Chalikov, D., 2005. "Fine scale inhomogeneity of wind-wave energy input, skewness, and asymmetry". *Geophys. Res. Lett.,* **32**(12), jun.

[40] Adcock, T. A. A., and Taylor, P. H., 2016. "Fast and local non-linear evolution of steep wave-groups on deep water: A comparison of approximate models to fully non-linear simulations". *Phys. Fluids,* **28**(1), jan, p. 16601.